

Condensation reactions of propanal over $Ce_xZr_{1-x}O_2$ mixed oxide catalysts

Anirudhan Gangadharan, Min Shen, Tawan Sooknoi¹, Daniel E. Resasco*, Richard G. Mallinson*

Center for Biomass Refining and School of Chemical, Biological and Materials Engineering, University of Oklahoma, Norman, OK, 73019, USA

ARTICLE INFO

Article history:

Received 10 March 2010

Received in revised form 22 June 2010

Accepted 25 June 2010

Available online 6 July 2010

Keywords:

Coupling

Aldol condensation

Ketonization

Biofuels

Ceria

Zirconia

Propanal

Mixed oxides

XPS

ABSTRACT

Vapor phase condensation reactions of propanal were investigated over $Ce_xZr_{1-x}O_2$ mixed oxides as a model reaction to produce gasoline range molecules from short aldehydes found in bio-oil mixtures. Several operating parameters were investigated. These included the type of carrier gas used (H_2 or He) and the incorporation of acids and water in the feed. Propanal is converted to higher carbon chain oxygenates on $Ce_xZr_{1-x}O_2$ by two pathways, aldol condensation and ketonization. The major products of these condensation reactions include 3-pentanone, 2-methyl-2-pentenal, 2-methylpentanal, 3-heptanone and 4-methyl-3-heptanone. It is proposed that the primary intermediate for the ketonization path is a surface carboxylate. The presence of acids in the feed inhibits the aldol condensation pathway by competitive adsorption that reduces the aldehyde conversion. Water also promotes ketonization and inhibits aldol condensation by increasing the concentration of surface hydroxyl groups that enhance the formation of surface carboxylates with the aldehyde. Hydrogen enhances cracking and production of light oxygenates and hydrocarbons. The light oxygenates may in turn be reincorporated into the reaction path, giving secondary products. However, the hydrocarbons do not react further. Analysis of the fresh and spent catalysts by XPS showed varying degrees of reduction of the oxide under different operating conditions that were consistent with the reaction results. Changing the proportion of the parent oxides showed that increased Zr favored formation of aldol products while increased Ce favored ketonization. This occurs by shifting the balance of the acid–base properties of the active sites.

© 2010 Elsevier B.V. All rights reserved.

1. Introduction

The production of fungible fuels from biomass offers a possible contribution to meet growing energy demands and to reduce their environmental impact. The conversion of solid biomass can be achieved through biochemical or thermochemical processes [1]. Biochemical processes involve fermentation of the biomass feedstock with a biological organism to produce ethanol or other products. Pyrolysis is a high temperature process that produces a liquid product that is commonly referred to as “bio-oil” [1]. Bio-oil is a complex mixture of a wide range of oxygenated compounds that include aldehydes, ketones, alcohols and carboxylic acids [2]. The catalytic conversion of glycerol that is obtained as a byproduct from the production of biodiesel also produces short aldehydes and acids [3]. The oxygenates found in bio-oil and from the conversion of glycerol can be converted to more suitable molecular weight

components as they possess reactive carbonyl moieties that can be used to carry out carbon–carbon bond forming reactions, thereby moving to the transportation fuel range while reducing the oxygen content of the oxygenate stream.

Ketonization and aldol condensation reactions are important routes in which aldehydes (or carbonyl containing species) can be converted into longer chain molecules. While ketonization produces higher ketones from aldehydes with the evolution of CO_2 and water, aldol condensation produces dimers and trimers of the corresponding aldehydes with the evolution of water. Previous studies on ketonization of oxygenates have been carried out on a variety of metal oxide catalysts that include CeO_2 , ZnO , TiO_2 , ZrO_2 , CeO_2/Mn_2O_3 , CeO_2/ZrO_2 and CeO_2/Fe_2O_3 [4–13,21–23,26–32].

It has been reported that ceria-based catalysts are active for ketonization of aldehydes, in which the aldehyde is oxidized to a carboxylate type species on the surface that then couples to produce the ketone [11,21,22,28–30,32]. Cerium oxide is known to possess a very high oxygen exchange capacity, due to its ability to alternate between Ce^{3+} and Ce^{4+} under reducing and oxidizing conditions, respectively [12,16–19,39]. The oxygen storage capacity of ceria has enabled its use as an oxygen carrier, but deactivation of ceria at high temperatures has led to the formulation of a new range of mixed oxides that have improved stability and redox properties [15,16]. The incorporation of ZrO_2 into the lattice of CeO_2 significantly changes the reducibility and oxygen storage capacity of the

* Corresponding authors at: University of Oklahoma, Chemical Engineering, 100 E. Boyd Street, Room T335, Norman, OK 73019, United States. Tel.: +1 405 325 4378; fax: +1 405 325 5813.

E-mail addresses: resasco@ou.edu (D.E. Resasco), mallinson@ou.edu (R.G. Mallinson).

¹ Permanent address: King Mongkut Institute of Technology Ladkrabang, Bangkok, Thailand.

oxide [16–19]. This has been attributed to changes to the fluorite structure of ceria and the creation of defects that increase oxygen mobility through the lattice [16–19]. In addition, the ceria–zirconia mixed oxides exhibit acid and base properties that can be utilized for both aldol condensation and ketonization reactions.

In this study, the ketonization and aldol condensation reactions of a representative short aldehyde, propanal, are carried out over a $\text{Ce}_{0.5}\text{Zr}_{0.5}\text{O}_2$ mixed oxide catalyst. The effects of different operating conditions have been tested, including changing the type of carrier gas used (H_2 or He) and incorporating short organic acids or water in the feed. A reaction pathway for the conversion of propanal is proposed and related to the structural properties of the catalyst. In addition, for comparison, changes in the ratio of the component oxides were studied.

2. Experimental

2.1. Catalyst preparation

$\text{Ce}_x\text{Zr}_{1-x}\text{O}_2$ mixed oxide catalysts were prepared by a co-precipitation method with aqueous solutions of cerium (IV) ammonium nitrate and zirconium nitrate as described in the studies by Hori et al. [18] and Noronha et al. [19]. Cerium (IV) ammonium nitrate and zirconium nitrate were dissolved in water in appropriate concentrations to have the required Ce/Zr ratio. Then the ceria and zirconia hydroxides were co-precipitated by increasing the pH through the controlled addition of ammonium hydroxide. The resulting solids were washed with deionized water, dried overnight in an oven and calcined at 773 K for 1 h. Pure CeO_2 and ZrO_2 were also prepared using the same method for comparison. γ -Alumina was purchased from Alfa Aesar and used as received.

2.2. Catalyst characterization

The catalysts were characterized by X-ray diffraction and temperature-programmed reduction (TPR).

The phase structure of the $\text{Ce}_x\text{Zr}_{1-x}\text{O}_2$ catalyst was investigated by X-ray diffraction (XRD) using a Rigaku Automatic diffractometer (Model D-MAX A) with a curved crystal monochromator and system setting of 40 kV and 35 mA. Data were collected in the angle range of 5–70° with a step size of 0.05° and a count time of 1.0 s. The samples were finely ground and placed on a glass slide using a smear mount technique.

TPR experiments were carried out in a gas mixture of 5% H_2 in Ar (25 ml/min) over a 30 mg catalyst sample. The temperature was increased from 303 K to 1223 K at 10 K/min. The effluent gases were analyzed using an online SRI 110 thermal conductivity detector (TCD). Prior to each TPR experiment, the sample was pretreated in 2% O_2 in He (30 ml/min) at 550 °C for 1 h.

2.3. X-ray photoelectron spectroscopy

X-ray photoelectron spectroscopy data were recorded on a Physical Electronics PHI 5800 ESCA system with monochromatic Al $K\alpha$ X-rays (1486.6 eV) operated at 100 W and 15 kV in a chamber pumped down to a pressure of approximately 1.0×10^{-8} Torr. A ~ 0.64 mm² spot size and 58.7 eV pass energy were typically used for the analysis. The electron takeoff angle was 45° with respect to the sample surface. The reduction and reaction of the samples were carried out in a fixed bed reactor with sealing valves at the top and bottom of the reactor. After each reaction experiment, the valves were closed and the reactor with the sample was transferred to a glove bag that was then purged with He to avoid any exposure to the atmosphere. The samples were removed from the reactor and

placed on a stainless steel holder and into an *ex situ* vacuum chamber within the bag and then kept in the vacuum chamber for the analysis. The XPS data from the regions related to C (1s), O (1s), Ce (3d) and Zr (3d) were recorded for each sample. The binding energies were corrected with reference to carbon at 284.8 eV. The reducibility of $\text{Ce}_x\text{Zr}_{1-x}\text{O}_2$ catalysts were evaluated by calculating the fraction of Ce^{4+} and Ce^{3+} in the samples by measuring the ratio of the area of the peak at 916.5 eV to the total area of the Ce (3d) spectrum, following a previously reported method [19,46,47].

2.4. Catalytic activity

The catalytic reactions were carried out in a 6 mm quartz tube reactor at atmospheric pressure at 400 °C. Prior to the reaction, the catalyst was reduced *in situ* in flowing H_2 (30 ml/min) at 400 °C. The feeds were propanal (from Aldrich), with, in some cases, propionic acid (from Aldrich) that were injected from a syringe pump into a heated port with a stream of flowing carrier gas (He or H_2). To test the effect of water addition with the feed, deionized water was injected with another syringe pump into the reactant line. Typical catalyst loads were 15–160 mg (40–60 mesh), with the feed and carrier flow rates adjusted to achieve the desired space time (W/F). All the lines were heated with heating tapes to keep the reactants and products in the gas phase. The products were analyzed and identified by online gas chromatography using an HP 5890 GC equipped with a flame ionization detector and a Shimadzu GC/MS, respectively. Analysis of the light hydrocarbon products was done using a Carle series 400 AGC equipped with TCD.

2.5. Temperature-programmed desorption (TPD) of propanal

In each TPD experiment, 50 mg of fresh catalyst sample was initially pretreated in flowing H_2 at 400 °C in the same diameter quartz tube as used in the continuous flow experiments. After pretreatment, the excess H_2 was removed by purging with He. 5 μl (liquid) of propanal was then repeatedly injected over the sample using a GC syringe (Hamilton 10 μl) at 400 °C until reaching saturation, as indicated by a steady MS signal. Excess propanal was removed by flowing He. The sample was then cooled down to room temperature in He and heated to 900 °C at a heating rate of 10 °C/min. Masses (m/z) of 16, 18, 28, 44 and 58 were monitored continuously by a Cirrus mass spectrometer (MKS) to determine the evolution of methane, water, carbon monoxide, carbon dioxide and propanal, respectively.

3. Results and discussion

3.1. Catalyst characterization

The textural properties of the oxides were characterized using X-ray diffraction (XRD). It is well known from the literature that pure CeO_2 exhibits a cubic phase while pure ZrO_2 shows a mixture of monoclinic and tetragonal phases [16,18–20]. The distinct peaks obtained for the mixed oxide samples in this study were consistent with those that have been reported previously in the literature [16,18–20] and these peaks can be assigned to contributions from both the CeO_2 and ZrO_2 phases. Shifts to higher angles were observed with increasing zirconia content in the sample, and are indicative of a change in the lattice parameter resulting from the incorporation of the smaller Zr^{4+} ion into the lattice of the larger Ce^{4+} ion.

The reducibility of the mixed oxides formed was characterized using temperature-programmed reduction (TPR) with H_2 . This technique has been widely used to characterize the reducibility of ceria-based materials in several previous studies and the results

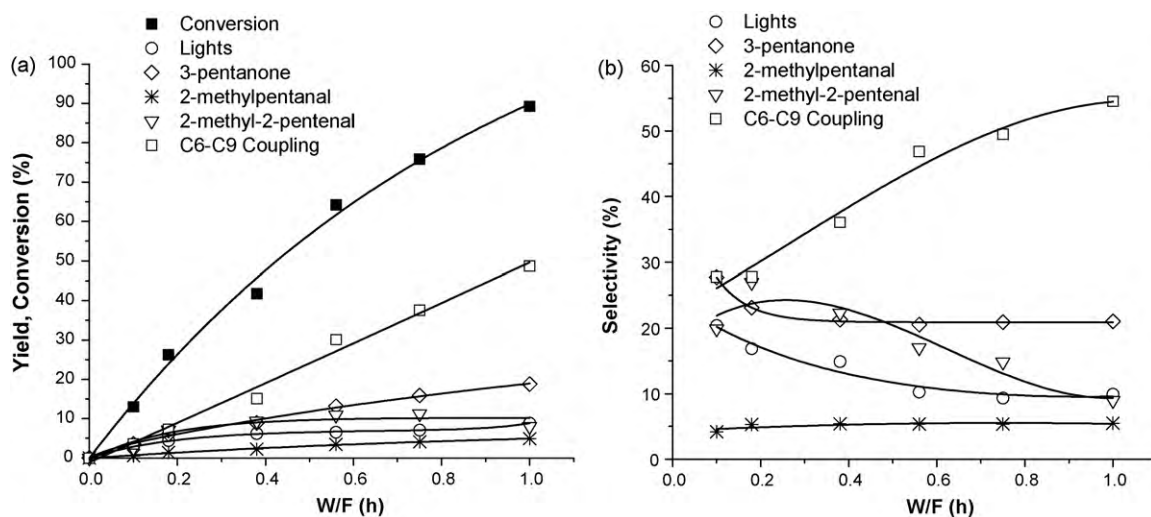


Fig. 1. Reaction of propanal as a function of W/F at 400 °C on Ce_{0.5}Zr_{0.5}O₂ in He. (a) Conversion and product yield. (b) Product selectivities.

obtained here are in agreement with those [16–20]. The TPR profile for pure CeO₂ showed two distinct regions, a low temperature region (300–600 °C) with a maximum at around 500 °C, attributed to the surface reduction of the Ce⁴⁺ ions and a high temperature region (700–900 °C), with a maximum at around 900 °C, originating from the reduction of the bulk oxide. The TPR profiles for the mixed oxides showed a single major reduction peak centered at temperatures between 500 and 600 °C. This result is indicative of the mixed oxide character of the catalyst and is due to the defects created by the insertion of Zr⁴⁺ into the lattice of Ce⁴⁺, as revealed by XRD, thus increasing the oxygen mobility through the lattice. As a result, the reduction now involves both the surface and bulk in a single step and also occurs at a much lower temperature compared to that of pure ceria. It is to be noted that there was no reduction of pure ZrO₂.

3.2. Product distribution as a function of W/F at 400 °C in helium

Fig. 1(a) shows the conversion and yields of products at different W/F from the conversion of propanal over the Ce_{0.5}Zr_{0.5}O₂ catalyst under He flow. The products obtained include a mixture of aldehydes (2-methylpropanal, 2-methyl-2-pentalenal, and 2-methylpentanal), ketones (2-butanone, 3-methyl-2-butanone, 2-methyl-3-pentanone, 3-pentanone, 3-heptanone, 4-methyl-3-heptanone, 4-methyl-3-heptenone and other higher ketones), hydrocarbons (methane, ethane, ethylene, propane, and propylene) and other light gases (CO and CO₂). Here, 2-methylpropanal, 2-butanone, 3-methyl-2-butanone and the hydrocarbons are reported as lights while 3-heptanone, 4-methyl-3-heptanone, 4-methyl-3-heptenone and other heavier ketones are reported as C₆–C₉+ coupling products.

From Fig. 1(a), it can be observed that 3-pentanone, 2-methyl-2-pentalenal and the C₆–C₉+ coupling products are the dominant products from the reaction. At low conversions (W/F < 0.2), the yields of 3-pentanone and 2-methyl-2-pentalenal are comparable, as observed from the slope of the curves. As the conversion increases, the yields of 3-pentanone, C₆–C₉+ products and 2-methylpentanal increase, while the yields of 2-methyl-2-pentalenal and lights reach a maximum and start to decrease, as shown in Fig. 1(a), suggesting that these are primary products. This can be seen more clearly in the plot of selectivity as a function of W/F, Fig. 1(b). A maximum in selectivity to the lights and 2-methyl-2-pentalenal is reached at around W/F of 0.1 and with a further increase in W/F, they decrease. It can also be seen that the selectivity to 3-pentanone reaches a

maximum at W/F of 0.1 and gradually decreases to a constant value with increasing W/F. The decreases in the yields and selectivities of 3-pentanone, 2-methyl-2-pentalenal and lights with increasing W/F indicate further reactions of these compounds to yield secondary products.

The formation of 3-pentanone on ceria-based catalysts has been reported previously in the literature [21,22,28,29,36]. Kamimura et al. [21,36] have proposed that the pathway to 3-pentanone from propanal is via an aldol addition intermediate, 3-hydroxy-2-methylpentanal, on CeO₂–MgO and CeO₂–Fe₂O₃ catalysts. They have reported that CO and CO₂ were evolved, consistent with a proposed oxidative decarboxylation of 3-hydroxy-2-methylpentanal on CeO₂–Fe₂O₃ and deformylation on CeO₂–MgO to give 3-pentanone. They also speculated that the extra oxygen necessary for the decarboxylation step comes from either water or an oxygen impurity in the carrier gas. However, Claridge et al. [22] have proposed that the extra oxygen in the ketonization to form 3-pentanone from propanal comes from the surface of the catalyst. Lietti et al. [23,26] have studied the reactions of C₃ oxygenates (1-propanol, propanal and propanoic acid), 3-pentanone and 2-butanone over ZnCrO_x and K₂O–ZnCrO_x catalysts using temperature-programmed reactions and flow experiments. A product distribution similar to the one obtained in this study was reported and a general reaction network was also proposed for the transformation of oxygenates over the ZnCrO_x catalyst that included hydrogenation-dehydrogenation, aldol condensation, ketonization, dehydration, decarboxylation and cracking reactions to yield the observed products [23,26].

Those previous studies have shown that propanal can either oxidize to a carboxylate type species on the surface and undergo further coupling to give 3-pentanone, or undergo aldol condensation to form the hydrated dimer (3-hydroxy-2-methylpentanal) that can decompose to give 3-pentanone. The former case requires lattice oxygen for the propanal to form a surface propionate species that then couples to give the ketone. Neither the hydrated dimer nor propionic acid was observed in the gas-phase as intermediate products over the ceria–zirconia catalyst in our study. CO₂ was the major gaseous product observed, while CO was seen only in trace amounts. Also, a steady decline in catalytic activity, to around one third of the initial activity was also observed (not shown here) over a 4 h reaction period, suggesting possible oxygen uptake from the surface. These results suggest that the formation of 3-pentanone over the ceria–zirconia catalyst occurs through a decarboxylative condensation reaction via a surface

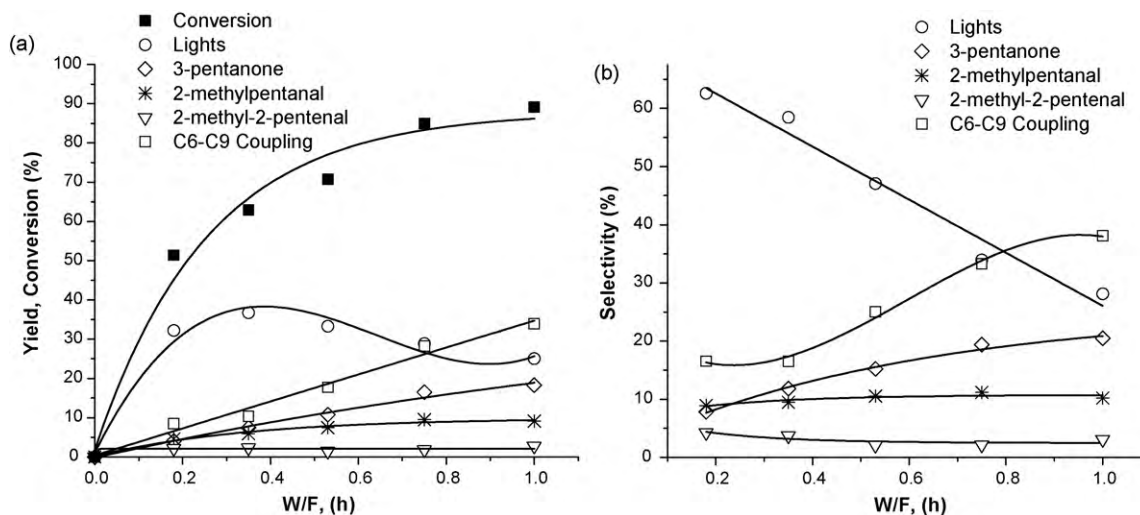


Fig. 2. Reaction of propanal as a function of W/F at 400 °C on Ce_{0.5}Zr_{0.5}O₂ in H₂. (a) Conversion and product yield. (b) Product selectivities.

propionate intermediate, using lattice oxygen. The aldol condensation pathway to give 2-methyl-2-pentalenal proceeds in parallel via the aldol addition dimer, 3-hydroxy-2-methylpentanal. The presence of additional products: 4-methyl-3-heptanone (ketonization), 2-methylpropanal, 3-heptanone (aldol condensation), 2-methyl-3-pentanone (reverse aldol condensation), 2-butanone and 3-methyl-2-butanone (reverse α -addition) and light hydrocarbons, CO and CO₂ (cracking, dehydration, and decarboxylation) in this study, are also consistent with the products observed by Lietti et al. [23,26]. To gain further insight into the reaction pathways, and also to understand the role of hydrogen, a similar series of experiments at different W/F were performed in a hydrogen atmosphere.

3.3. Product distribution as a function of W/F at 400 °C in hydrogen

Hydrogen creates a reduced surface of the oxide, where the coordination environment of the surface cation is altered to give a broad distribution of cation oxidation states. Hydrogen is adsorbed on the surfaces of ceria-zirconia as chemisorbed H atoms. These H atoms interact with surface oxygen to form hydroxyl groups on the surface. These surface hydroxyl groups subsequently interact with hydrogen and desorb as H₂O, creating an oxygen vacancy and the reduction of Ce⁴⁺ species. FT-IR spectroscopic studies [45] have shown that there is an increase in the intensity of the OH band up to the reduction temperature, above which there is a decrease due to the formation of water and oxygen vacancies on the surface. In the same study, results from magnetic balance experiments showed that the reduction percentage of ceria was much higher at a lower temperature for the mixed oxides, compared to the pure oxide [45], implying that the mixed oxides are more easily reduced compared to the pure oxide. The removal of oxygen in this process creates Lewis acidity [45] that might be helpful for ketonization. In addition, hydrogen can also promote hydrocracking or hydrogenolysis reactions. Also, if ketones and aldehydes are hydrogenated, dehydration/hydrogenation is an effective deoxygenation path (in this case undesirable) that results in generation of light hydrocarbons.

Fig. 2 shows the product distribution obtained at different W/F over the Ce_{0.5}Zr_{0.5}O₂ catalyst under hydrogen flow. As can be seen from Fig. 2(a), the yield of light hydrocarbons is increased by a significant amount in the presence of hydrogen. The lights reach a maximum between W/F of 0.2 and 0.4 and then decrease gradually with increasing W/F. As mentioned above, it is easy to see that hydrogen can favor formation of light hydrocarbons and oxygenates, through cracking and dehydration but the decrease

in the yield of these products at longer W/F suggests that these compounds may be further converted to secondary products. The changes in product selectivities as a function of W/F (Fig. 2(b)) further highlight the decrease in lights at higher W/F with a corresponding increase in the C₆–C₉ coupling products.

The yield of 3-pentanone in H₂ is comparable to that obtained in He. The yield of 2-methylpentanal, that is formed by the hydrogenation of 2-methyl-2-pentalenal, is increased while there is a significant decrease in the yields of 2-methyl-2-pentalenal and the C₆–C₉+ ketonization products.

3.4. Proposed reaction network

In order to better understand the possible secondary reactions that modify the product distribution, some of the possible intermediate products and co-products were fed over Ce_{0.5}Zr_{0.5}O₂ in He or H₂ flow under similar reaction conditions as those used with the propanal feed. These results are summarized in Table 1.

3.4.1. Feeding oxygenates

Experiments using 2-methyl-2-pentalenal as the feed, with either H₂ or He as the carrier, showed that the resulting major products from this dimer were 2-methylpentanal and light hydrocarbons, with very low yields of the heavier ketones (Table 1). While the overall conversion of this C₆ aldehyde was much higher under H₂ than under He for the conditions tested, the products obtained with H₂ and He were comparable to those obtained with propanal. The higher yields of lights and 2-methylpentanal obtained with H₂ are also comparable to those with propanal as the feed. This result suggests that the majority of the lighter compounds are formed from 2-methyl-2-pentalenal and also confirms the reason for the decrease in the yield and selectivity of 2-methyl-2-pentalenal as a function of W/F in H₂ and in He, as shown in Figs. 1 and 2.

An experiment with 3-pentanone as the feed in He showed that the main reaction products were 2-butanone, 3-methyl-2-butanone, 2-methyl-3-pentanone, 3-heptanone, 4-methyl-3-heptanone and other heavier ketones. The conversion of this C₅ ketone was much lower than either propanal or 2-methyl-2-pentalenal under the tested conditions, as shown in Table 1. The ketones in the products from the reaction of 3-pentanone are comparable to those obtained from propanal. This exhibits the ability of 3-pentanone to participate in additional condensation reactions to give the observed products and also explains the gradual decrease observed in its selectivity as a function of W/F in He (Fig. 1(b)).

Table 1
Product distribution from the reaction of oxygenates over $\text{Ce}_{0.5}\text{Zr}_{0.5}\text{O}_2$ on a CO_x and H_2O free basis, TOS 15 min.

Feed	Carrier gas	Temperature, °C	W/F, h	Conversion (%)	Products	Selectivities (% wt)
2-Methyl-2-pentenal	He	400	0.37	42.6	Lights ^a	53.2
					2-Methylpentanal	24.2
					Heavies	22.5
2-Methyl-2-pentenal	H_2	400	0.37	96.3	Lights ^a	69.9
					2-Methylpentanal	20.0
					Heavies	10.0
3-Pentanone	He	400	0.40	13.0	Lights ^a	17.5
					2-Methyl-3-pentanone	21.5
					2-Butanone	9.1
					Other coupling ketones ^b	51.9

^a Hydrocarbons and oxygenates.

^b 3-Heptanone, 4-methyl-3-heptanone, 4-methyl-3-pentanone and other higher ketones.

The results from the experiments with 2-methyl-2-pentenal and 3-pentanone as the feeds indicate that the same types of chemical reactions and catalytic functions are operative with each of the feeds over this catalyst. The presence of significant amounts of hydrocarbons from the reactions of 3-pentanone and 2-methyl-2-pentenal shows that hydrogenation to the corresponding alcohols and subsequent dehydration to give the light hydrocarbons is occurring.

Experiments with ethylene and propylene fed to this catalyst were conducted to test the reactivity of the light olefins towards incorporation into oxygenates. Previous studies have shown that light gases like ethane, ethylene, and propylene can convert to

oxygenated compounds on several mixed oxide catalysts by taking up oxygen by an oxidative dehydrogenation (ODH) reaction [24]. However, no appreciable conversion was observed under the conditions tested, further confirming that the light oxygenates (2-methylpropanal, 2-butanone, and 3-methyl-2-butanone) are the reacting species.

Based on these results, the reaction network shown in Fig. 3 is proposed to account for the formation of the products observed experimentally. The network contemplates the contribution of two major reactions, aldol condensation and ketonization, which in turn involve various condensation steps. In addition, there are also several side reactions that can take place in parallel. First, it is

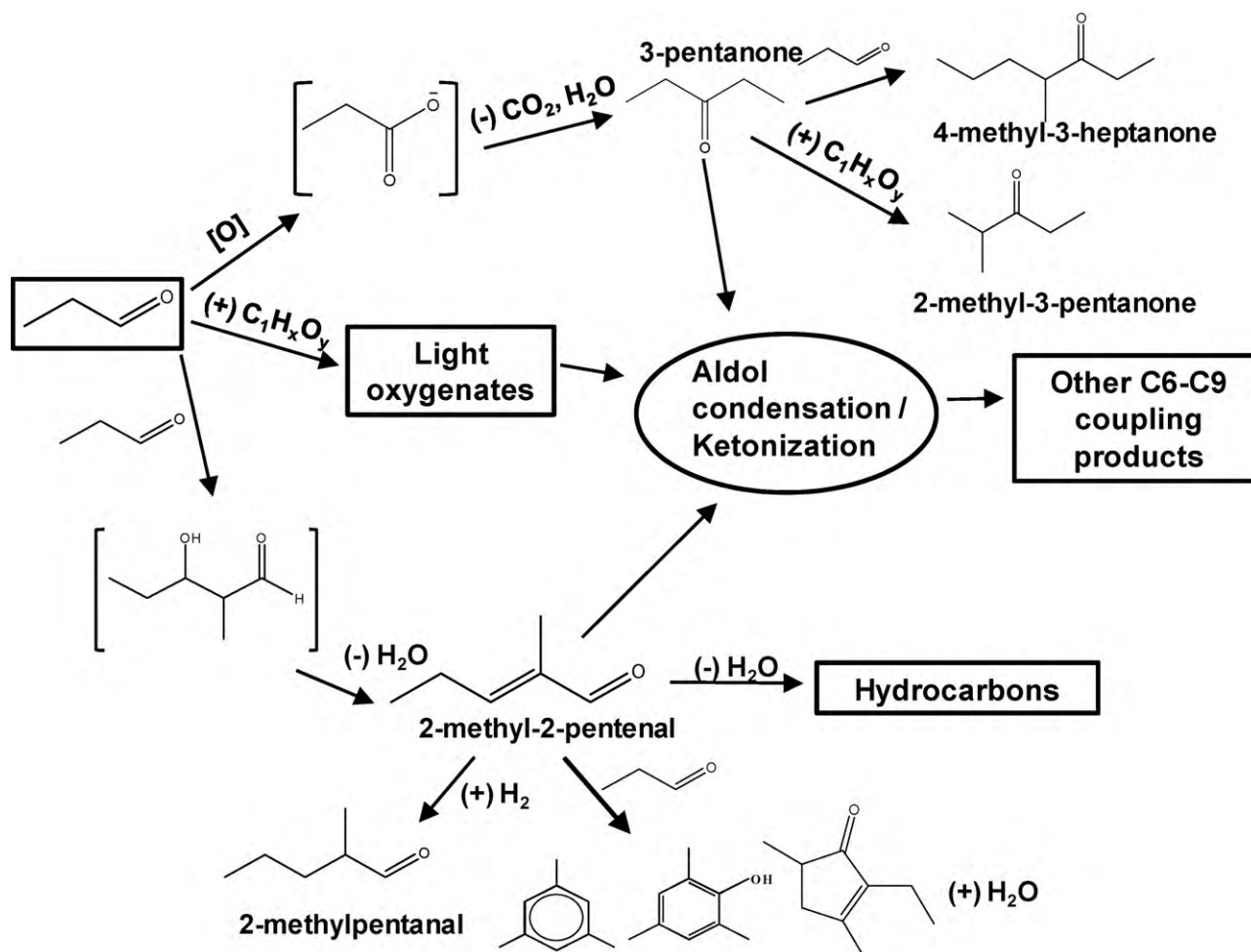
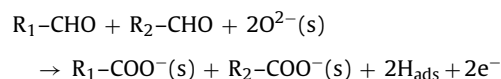


Fig. 3. Proposed reaction pathway of propanal conversion over $\text{Ce}_{0.5}\text{Zr}_{0.5}\text{O}_2$.

known that aldol condensation can occur on both acid and basic sites [25]. In the mixed oxides, the exposed cations are Lewis acid sites while the oxygen anions can act as either Lewis or Bronsted base sites. Aldol condensation of aldehydes does not require multiple coordination of surface cations, but involves the reaction of an adsorbed conjugate base anion with an adsorbed molecule (ion-molecule reaction) to form a β -hydroxyaldehyde that subsequently dehydrates to give the higher aldehydes or ketones [12]. The aldol condensation of propanal via the hydrated dimer (3-hydroxy-2-methylpentanal), produces 2-methyl-2-pentenal that is subsequently hydrogenated to 2-methyl-pentanal and may also crack to give some lighter compounds. The aldol condensation can proceed further to give the cyclic trimers of propanal that include mesitylene, 2,4,6-trimethylphenol and 2-ethyl-3,5-dimethylcyclopent-2-en-1-one. However, the trimers are only minor products and are included here for completeness.

In addition to producing the dimers and trimers of propanal, aldol condensation can also give rise to several other products observed here. Studies over a ZnCrO_x catalyst [23,26] with C_3 – C_4 oxygenates as the feed have reported a wide range of aldehydes and ketones as the products. It was also shown in that study that some of the short aldehydes and ketones produced could react further to give longer chain products. They have also classified the reactivities of these short carbonyl species based on their molecular structure and have considered them either as electrophilic or nucleophilic reactants. Hence, as also included in Fig. 3, the source of the formation of some of the observed products can be explained as follows: 3-heptanone from propanal + 2-butanone, 4-methyl-3-heptanone from propanal + 3-pentanone, 3-methyl-2-butanone from formaldehyde + 2-butanone, 2-methyl-3-pentanone from 3-pentanone + formaldehyde. It is to be noted that in the above reactions, ketones act as the nucleophilic species. The formation of 2-butanone and formaldehyde will be discussed later.

It is proposed that the ketonization pathway proceeds with oxidation of propanal on the surface to give a propionate intermediate, which then couples to give the symmetric ketone (3-pentanone). Oxidation reactions are common on the surfaces of oxides [25,27]. The oxide anions, which are Lewis or Bronsted bases, can transform the adsorbed carbonyl groups to the corresponding surface carboxylates by nucleophilic attack at the carbonyl carbon of the substrate by surface oxygen according to the following:



Further reaction of these adsorbed carboxylates to form the coupled ketones occurs by:



The above reaction is highly dependent on the availability of potential reaction partners, which in turn is dependent on the coordination environment of the surface cation and the redox properties of the oxide. Ceria has the highest surface oxygen mobility compared to other single oxides and the incorporation of zirconia into the lattice of ceria enhances this surface oxygen mobility and thus the reducibility of the mixed oxide [16,18,19].

Therefore, with the improvement in the oxygen storage capacity of the mixed oxide, the tendency to form surface carboxylates to give coupled ketones on $\text{Ce}_{0.5}\text{Zr}_{0.5}\text{O}_2$ is greater than that expected for a pure oxide. The oxygen vacancy created after decarboxylative ketonization is replenished by the transport of oxygen from the bulk, according to the Mars Van Krevelen mechanism. This property of the mixed oxide is also believed to play an important role in catalyzing the reactions to the higher ketones. Plint et al. [27] have proposed such a carboxylate mechanism for forming 4-heptanone from 1-butanol over a CeO_2/MgO catalyst. They have

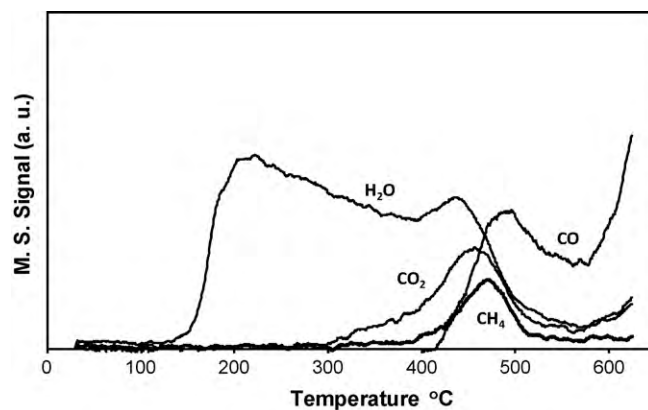


Fig. 4. Evolution of products from pre-adsorbed propanal over $\text{Ce}_{0.5}\text{Zr}_{0.5}\text{O}_2$ as a function of temperature, using He as carrier gas.

shown that the pathway to 4-heptanone involves the oxidation of the alcohol to the aldehyde and subsequently to the acid, which in turn forms surface carboxylates that couple to give the ketone. These authors also reported that the oxygen required for the oxidation steps comes from ceria. In addition, Kobune et al. [28] have reported the formation of 3-pentanone and the higher coupled ketones on CeO_2 and $\text{CeO}_2\text{-Fe}_2\text{O}_3$ catalysts and mentioned various stepwise condensation reactions to form the higher ketones. Hence, the presence of some ketones observed as the products in this study can be explained by the following ketonization reactions: 3-pentanone from propanal + propanal, 4-methyl-3-heptanone from propanal + 2-methylpentanal, 3-methyl-3-pentanone from propanal + 2-methylpropanal and so on.

The presence of light oxygenates like 2-butanone, 2-methylpropanal and 3-methyl-2-butanone in the product stream from the conversion of propanal shows that, in addition to aldol condensation and ketonization, there can be other side reactions taking place to give these products. Lietti et al. [23] have suggested that a C_1 oxygenated intermediate, possibly formaldehyde, could be involved in the formation of these products, but that product has not been detected. The origin of the formaldehyde species could be from the hydrogenation of CO_2 , produced from ketonization reactions by surface hydrides.

The temperature-programmed desorption (TPD) study of propanal adsorbed over ceria-zirconia is shown in Fig. 4. Three main peaks, between temperature $T=400$ – 500 °C are evident and are associated with methane, CO_2 and CO. The evolution of methane and CO_2 at the same temperatures indicates the possibility of surface formate species being involved in the reaction. The formation of surface formate species over ceria-based catalysts has been reported by Barteau and co-workers [11]. Hence, the formation of 2-butanone probably occurs via an α -addition reaction between propanal and formaldehyde, while 2-methylpropanal is formed via a cross-aldol condensation between propanal and formaldehyde and 3-methyl-2-butanone is formed through a reverse α -addition between 2-methyl-propanal and formaldehyde, as indicated in Fig. 3. The desorption of water can be observed between $T=150$ – 500 °C, as a by-product of aldol condensation, ketonization and dehydration reactions.

3.4.2. Effect of addition of acid and water

The role of acids in the overall reaction pathway was examined using propionic acid as a model feed. Self-condensation of acids on oxide catalysts gives symmetric ketones, while cross-condensation between two different acids can give two symmetric ketones (one from each acid) as well as an asymmetric ketone [29,30]. A number of studies have shown that a wide range of oxides, including CeO_2 ,

Table 2
Effect of incorporating water or propionic acid in the feed on product distribution over $\text{Ce}_{0.5}\text{Zr}_{0.5}\text{O}_2$ catalyst, He gas carrier, 400 °C, 1 atm, TOS 15 min.

Feed	Propanal	Propanal + propionic acid	Propanal + water
W/F, h	0.35	0.38	0.35
Feed: additive ratio (by wt)	–	5–1	4–1
Aldol products/3-pentanone ratio	1.4	0.5	0.5
Aldol products/coupling ketones ratio	0.5	0.3	0.2
<i>Product yields (%wt)</i>			
Lights	5.6	4.7	4.3
<i>Aldol products</i>			
2-Methylpentanal	2.3	2.2	2.3
2-Methyl-2-pentenal	9.4	6.8	5.2
1,3,5-Trimethyl benzene	0.1	0.1	0.1
2,4,6-Trimethyl phenol	0.6	0.8	0.8
2-Ethyl-3,5-dimethyl-2-cyclopent-2-en-1-one	0.3	0.3	0.2
<i>Coupling ketones</i>			
3-Pentanone	9.0	19.0	15.5
3-Heptanone	1.8	2.4	3.3
4-Methyl, 3-heptanone	1.6	1.9	2.1
2-Methyl, 3-pentanone	1.0	1.4	1.6
4,4,6-Trimethyl-2-cyclohexen-1-one	0.9	1.2	1.1
Other coupling products	9.1	11.4	13.2

are active for ketonization of acids [31–33]. Some studies have also reported that solid solutions of ceria-based oxides were the most active for the ketonization of acids [7,30].

Fig. 5 shows the conversion of propanal as a function of TOS, comparing an experiment using pure propanal as feed to another one using a mixed feed of propanal and propionic acid (5:1 mass ratio). No acids were detected in the products in the co-feed experiments, showing that the reaction of the acid on the surface of the oxide to form ketones is very fast. Fig. 5 also shows that, with the co-feed of propionic acid, the conversion of propanal was reduced significantly. The deactivation of the catalyst was more severe for the feed with acid incorporated than for the pure propanal feed. Table 2 shows the yields of the products obtained in both experiments at the shortest TOS. Here, the aldol products are the dimers and trimers from the self-condensation of propanal, while the coupled ketones are all the other observed ketones. The results show a significant increase in the yield of 3-pentanone with the addition of propionic acid and also an increase in the yields of the coupled ketones. However, a decrease in the yields of 2-methyl-2-pentenal (aldol dimer) and lights are observed. Also, the ratio of aldol products to 3-pentanone and the ratio of aldol products to the coupled

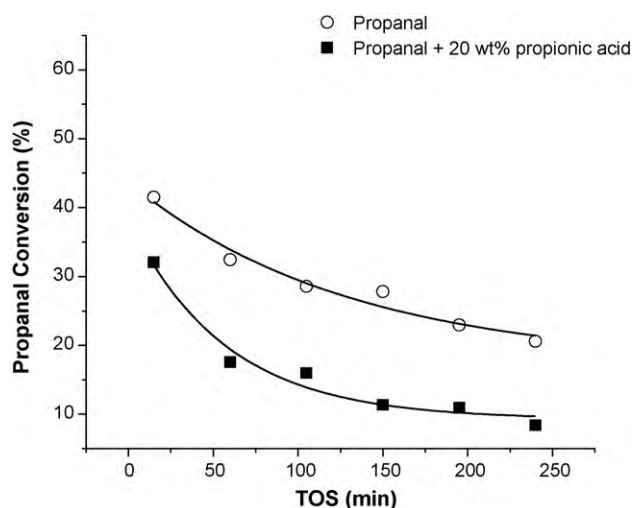


Fig. 5. Effect of addition of acid on propanal conversion over $\text{Ce}_{0.5}\text{Zr}_{0.5}\text{O}_2$. Reaction conditions: 400 °C, 1 atm, He.

ketones, shown in Table 2 decrease by a significant amount as compared to the feed with pure propanal. This implies that there is competitive adsorption of the aldehyde and acid on the surface, on which the acids are preferentially adsorbed. As a result, the number of sites available for the adsorption and reaction of propanal are reduced, producing its lower conversion and fewer aldol products. In agreement with this description, an additional experiment with a mixed feed of 1:1 mass ratio of acid and aldehyde gave an even higher proportion of ketonization products compared to aldol products, i.e., a ratio of about 16, while the overall propanal conversion was further reduced.

From previous studies in the literature, it has been shown that acids undergo self and cross-condensation reactions to give symmetric and asymmetric ketones at relatively low temperatures [29]. Thus, it is expected that with the addition of acids there will be a significant increase in the yield of 3-pentanone (symmetric ketone from propionic acid). However, the results show that acids can also undergo other parallel reactions leading to an increase in the yields of the coupled ketones (Table 2). Nagashima et al. [29] have studied the reactivity of propionic acid with various branched and linear carboxylic acids over CeO_2 based mixed oxides. They reported that with propionic acid and another carboxylic acid, three ketones were obtained; 3-pentanone from propionic acid, the symmetric ketone from the other acid, and the corresponding asymmetric (cross-condensation) ketone. This is in agreement with our results, where with the addition of propionic acid, we see an increase in the yield of the symmetric ketone as well as an increase in the yields of the other coupling products. These coupling products are mainly higher ketones and are grouped together in the table for simplicity.

Hence, the observed increase in the yields of ketones upon acid incorporation can be attributed to an increase in the amount of carboxylate type species on the surface and also results in an increase in the amount of CO_2 produced from the increased ketonization.

With more CO_2 produced, there is a possibility of forming higher amounts of formaldehyde and subsequently increases in the amounts of 2-butanone and 2-methylpropanal. These species can then undergo aldol condensation and ketonization reactions, as discussed in the previous section, and hence contribute to an increase in the yields of the higher ketones. However, with an increase in the carboxylate type species on the surface, it is possible that these can promote a variety of cross-condensation reactions, in addition

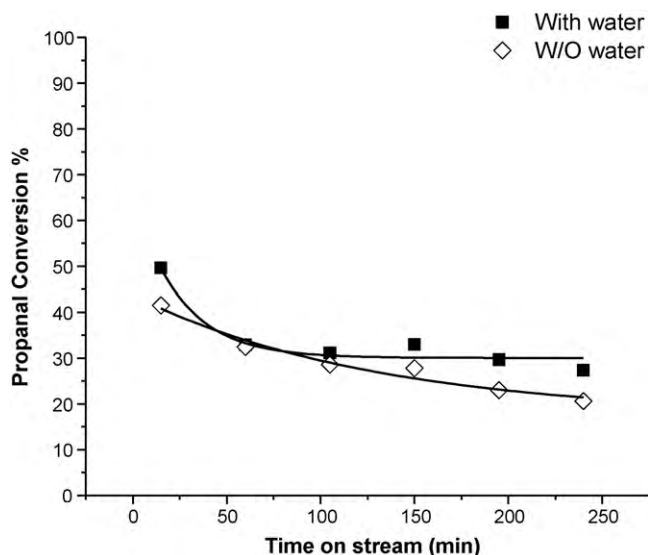


Fig. 6. Effect of water on propanal conversion over $\text{Ce}_{0.5}\text{Zr}_{0.5}\text{O}_2$. Reaction conditions: 400°C , 1 atm, W/F 0.35 h, He, F_{propanal} 0.2 ml/h, F_{water} 0.04 ml/h.

to self-coupling that forms the symmetric ketone. This provides an explanation for the observed increase in yield of coupling products, as well as their complexity.

Water is a byproduct from both aldol condensation and ketonization reactions and is believed to play an important role in promoting ketonization reactions on oxides. Studies of oxidation of hydrocarbons on metal oxide catalysts [24] and benzaldehyde reactions on oxide catalysts [35] have shown that water enhances the oxidation of the aldehydes to the corresponding acids. This is because, in the presence of water molecules, the concentration of the surface hydroxyl species is increased and these hydroxyl species facilitate the attack at the carbonyl carbon of the substrate by the lone pair of electrons on the oxygen atom to form the corresponding carboxylates on the surface that subsequently desorb as acids.

Fig. 6 shows the conversion of propanal as a function of TOS for feeds with and without water. It can be seen that the conversion and stability of the catalyst are improved with the addition of water. The improvement in stability may be because water acts as a source of oxygen that helps to desorb products from the surface and also promotes the oxidation of coke, thus creating more active sites for the reaction to proceed. Table 2 shows the yields of the products obtained for this experiment, together with the results for the experiments with pure propanal and the propionic acid co-feed experiment. A similar effect, as with the addition of acid, is observed here with water. There is a significant increase in the yield of 3-pentanone and also an increase in yields of the C_6 – C_9 coupling products with a corresponding decrease in the yields of 2-methyl-2-pentenal and lights, while there is not much change in the small yields of the higher aldol

condensation products. The ratios of aldol products to 3-pentanone and the coupling ketones also show a decrease with the feed with water.

Water is adsorbed on the surface of oxides as H and OH groups (dissociative chemisorption). These surface hydroxyl groups are moieties that can initiate nucleophilic attack by oxygen at the carbonyl carbon of the aldehydes to form the corresponding acids [24,35]. In the presence of water with propanal over the ceria–zirconia catalyst, the surface hydroxyl groups can increase the transformation of the adsorbed propanal to the surface propionate species, as depicted in Fig. 7. The surface propionate can then couple with another similar species and desorb as the symmetric ketone or react further with other surface species via the pathways shown in Fig. 3 to give the observed increase in the yields of the products in the presence of water. However, it should be noted that with increasing partial pressure of water, it is very likely that the reaction would eventually be inhibited by blocking of the active sites by adsorbed water molecules. Therefore, the effect of water on the ketonization activity is a balance between the availability of O^{2-} anions as well as the extent of hydroxylation of the surface, since an oxygen anion is required for the abstraction of an H atom to form the propionate species. Yokoyama et al. [35] have reported that, with benzaldehyde and water vapor in the feed over ZrO_2 and $\text{Cr}_2\text{O}_3/\text{ZrO}_2$ catalysts, benzaldehyde forms a benzoate species on the surface with the lattice oxygen. A surface hydroxyl group then attacks the carboxyl group of the benzoate species to produce benzoic acid and hydrogen as the observed products. That study further supports the results observed here.

In summary, these results have shown the integral role played by acids and water in altering the reaction pathway; the addition of acids or water suppresses aldol condensation and promotes ketonization. While addition of acid reduces the conversion of propanal, addition of water increases the conversion and enhances the catalyst stability over time.

3.4.3. XPS analysis of fresh and spent catalysts

The reaction experiments performed thus far have suggested that the ketonization of propanal over the ceria–zirconia mixed oxides occurs through the oxidation of propanal on the surface to form surface carboxylates and further reactions of these carboxylate type species give 3-pentanone and higher ketones. The key step to these reactions, as discussed in the previous sections, is the formation of the carboxylate intermediate on the surface and this suggests that the oxygen from the surface of the mixed oxide participates in this reaction. In doing so, the cerium would shift between the Ce^{4+} and Ce^{3+} states to create oxygen vacancies. Therefore, it is of interest to determine the nature of the surface and the oxidation states of the elements before and after reaction. Therefore, a series of experiments were performed with the catalyst samples being treated under different conditions. The catalyst samples analyzed were: (i) fresh, (ii) reduced at 400°C , (iii) after reaction of propanal in H_2 , (iv) after reaction of propanal in He, (v) after reaction of propanal with co-feed of propionic acid, (vi) after reaction of propanal with co-feed of water.

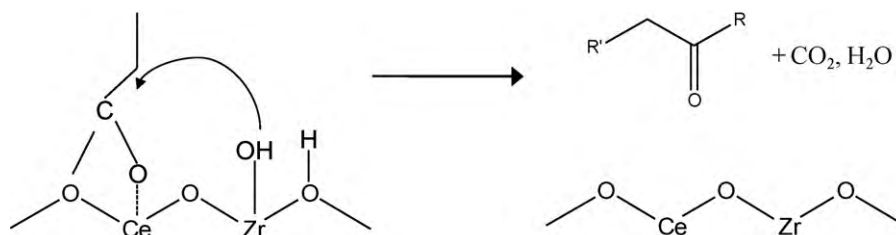


Fig. 7. Schematic of the interaction of adsorbed water with propanal.

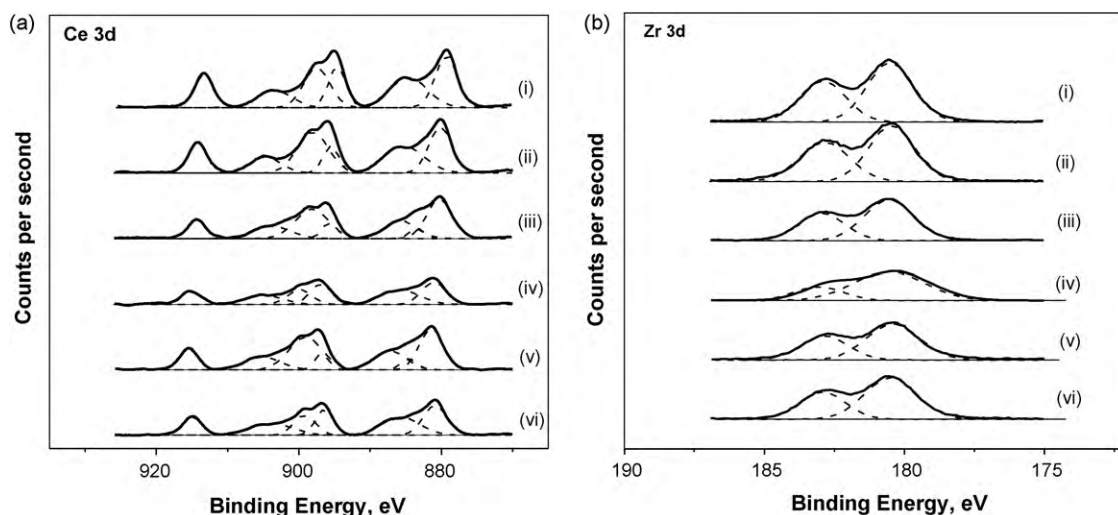


Fig. 8. (a) Ce (3d) and (b) Zr (3d) XPS spectra for $\text{Ce}_{0.5}\text{Zr}_{0.5}\text{O}_2$ treated under different conditions: (i) fresh catalyst, (ii) catalyst reduced at 400 °C, (iii) reaction in H_2 , (iv) reaction in He, (v) reaction with co-feed of acid, and (vi) reaction with co-feed of water.

Fig. 8 shows the XPS spectra of Ce (3d) and Zr (3d) regions of the samples from these experiments. It can be observed that the Ce (3d) spectrum is composed of several peaks and the complexity of the spectrum is reported as being due to the hybridization between the partially occupied 4f levels of ceria and the 2p states of oxygen [19,46–49]. The spectrum was fitted with up to eight peaks with Gaussian distributions and the main peaks and satellites were identified and labeled according to those used by Burroughs et al. [14]. Peaks denoted as u and v correspond to $3d_{3/2}$ and $3d_{5/2}$ contributions, respectively, while peaks with primed labels denote satellite features. The peaks v , v' , and v'' (and correspondingly for u) are attributed to Ce^{4+} , while v' and u' are attributed to Ce^{3+} . The spectrum of the Zr (3d) region shown in Fig. 8(b) consists of Zr $3d_{3/2}$ and Zr $3d_{5/2}$ primary ionization features and was fitted with two Gaussian curves.

In Fig. 8(a), it can be seen that there is a shift to higher binding energies in the Ce (3d) spectrum as the treatment conditions change from fresh catalyst to the one with reaction in He. There also seems to be a slight shift to lower binding energies for the one with the co-feed of water. This shift in the positions of the Ce (3d) band is indicative of a change in the coordination environment of the Ce atoms and could possibly be due to a combination of electronic and morphological changes. Therefore, it is conservative to determine the oxidation states on the surface on the basis of the method reported in a number of works in the literature [19,46,47]. By this method, the ratio of the area of u'' satellite peak relative to the total area under the Ce 3d spectrum was calculated, since the u'' does not overlap with the other peaks in the spectrum. This ratio then corresponds to the % Ce^{4+} (or Ce^{3+}) in the samples. Table 3 shows the % u'' and the % of Ce^{3+} estimated from the XPS analysis of the samples. It can be seen that the fresh ceria–zirconia catalyst had the lowest value of the % Ce^{3+} of 7 and the reduction of this sample in

H_2 at 400 °C increased this value to 10. The increase in the value of % Ce^{3+} is expected since reduction in H_2 creates oxygen vacancies and decreases the oxidation state of cerium. The reaction of propanal in H_2 at 400 °C increased this value to 29, while for the same reaction under He, the increase was only to 18. The differences observed with H_2 and He are explained in terms of the reacting environment under the two carrier gases. The surface is more deficient in oxygen with H_2 as the carrier and with the reactions of propanal, both consume oxygen (H_2 creates oxygen vacancies, while reacting surface species require coordination to oxygen) and therefore create lower oxidation state Ce ions. However, with He as the carrier, the oxygen is removed only by the reacting species and the amount of Ce^{4+} reduced is lower.

With the co-feeds of water and propionic acid, it is expected that the reduction of the oxide will be less compared to the pure propanal feed, as the surface will be enriched in oxygen by the presence of oxygen containing molecules (propionic acid and water) in the feed, in addition to propanal. From Table 3, it is clear that the reaction with co-feed of water exhibited this effect, as the value of % Ce^{3+} is much lower (14) compared to the other conditions and is closer to the value of the reduced sample. This is consistent with the results reported in Section 3.4.2 for co-feed of water and supports the proposed observation that water promotes the oxidation of propanal. With the co-feed of acid, the increase in the value of % Ce^{3+} (23) could be due to further reactions initiated in the presence of acids on the surface, leading to a more reduced surface of the oxide. This is also in agreement with the results from Section 3.4.2, where with the addition of acid in the feed, there was an increase in the yields of the coupling products. In summary, these results have shown that the state of reduction of the mixed oxide under different reaction conditions support the results observed in the steady state runs.

3.4.4. Effect of changing the composition of the mixed oxides

The changes in acid–base properties of mixed oxide catalysts with the change in the composition have been reported in previous studies [7,32–34,37,38]. The incorporation of ZrO_2 into the fluorite structure of CeO_2 can significantly change the acid–base properties of the mixed oxide in addition to improving the oxygen mobility through the lattice [13,15–19,40,41]. This property of the mixed oxide catalyst has been studied here with the condensation reactions of propanal and the results obtained are discussed based on the structural properties of the different catalysts.

Table 3
Percent of u'' and Ce^{3+} from XPS analysis.

	u'' in Ce (3d) (area%)	Atomic Ce^{3+} (%)
Fresh CZ 50	12.26	7
CZ 50 reduced at 400 °C	11.83	10
CZ 50 reaction in H_2	9.29	29
CZ 50 reaction in He	10.84	18
CZ 50 reaction with co-feed of acid	10.08	23
CZ 50 reaction with co-feed of water	11.37	14

CZ 50— $\text{Ce}_{0.50}\text{Zr}_{0.50}\text{O}_2$.

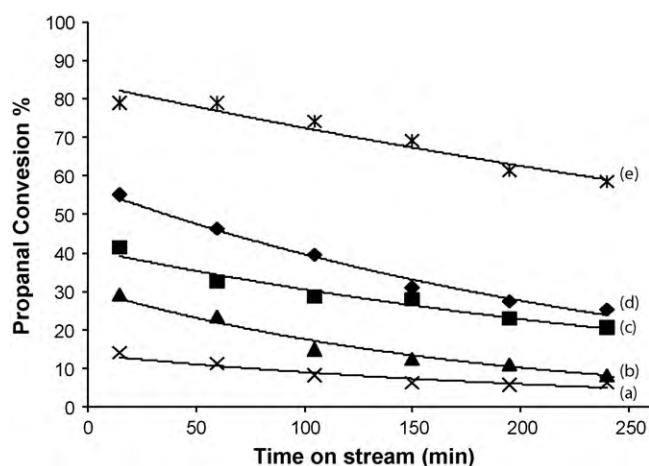


Fig. 9. Effect of changing the composition on propanal conversion over (a) CeO₂, (b) Ce_{0.75}Zr_{0.25}O₂, (c) Ce_{0.5}Zr_{0.5}O₂ and (d) Ce_{0.25}Zr_{0.75}O₂ (e) ZrO₂. Reaction conditions: 400 °C, 1 atm, W/F 0.35 h, He.

The catalysts tested were ZrO₂, Ce_{0.25}Zr_{0.75}O₂, Ce_{0.5}Zr_{0.5}O₂ and Ce_{0.75}Zr_{0.25}O₂ and CeO₂. The mixed oxides will be referred to as Ce–Zr (25–75), Ce–Zr (50–50) and Ce–Zr (75–25), respectively. Fig. 9 shows the conversion as a function of TOS over the catalysts under helium flow. It can be observed that, with the same space time (W/F) of 0.35 hr, pure zirconia exhibited the highest activity for the conversion of propanal, followed by Ce–Zr (25–75) > Ce–Zr (50–50) > Ce–Zr (75–25) > pure ceria. The higher activity observed with catalysts with higher zirconia content could be due to the nature of the sites present in the catalyst that favor either aldol condensation or ketonization reactions. This will be discussed in detail below. The deactivation profile looks similar for all the catalysts over a 4 h reaction period. Table 4 compares the product yields for the reaction of propanal over the five catalysts. The space time (W/F) was adjusted so that a similar level of conversion was achieved for all the catalysts for comparison. With a change in the composition of the oxides, a significant change in the product distribution is observed. In Table 4, from left to right, the catalysts have increasing zirconia content (reduced ceria content) and it can be seen that with an increasing amount of zirconia, there is a significant increase in the yields to 2-methyl-2-pentenal (aldol dimer) and other aldol condensation trimers with a corresponding decrease in the yields to 3-pentanone. Similarly, with an increasing ceria content (right to left in Table 4), the 3-pentanone formation is promoted while aldol condensation reactions are reduced. The

Ce–Zr (50–50) catalyst shows a balance in catalyzing both aldol condensation and ketonization reactions. In addition, the comparison between aldol condensation and ketonization was tested with a non-reducible oxide, γ -alumina. The results obtained with γ -alumina are comparable with those obtained with ZrO₂ and Ce–Zr (25–75), as shown in Table 4. The major product observed is the aldol dimer, 2-methyl-2-pentenal, with only small yields to 3-pentanone.

The results obtained here show that, by varying the ceria and zirconia content of the mixed oxide catalyst, the selectivity towards either aldol condensation or ketonization can be increased. This can be explained in terms of the nature of the active sites required for the reactions. Aldol condensation requires a basic site for the extraction of an α -hydrogen to form an enolate species and then subsequent dimerization giving the aldol dimer and other condensation products. FTIR studies of CO₂ adsorbed on ceria–zirconia mixed oxide catalysts [42] were performed to show that ceria–zirconia mixed oxides possess weak, medium and strong basic sites that corresponding to OH[−], M–O^{2−} and low coordinating O^{2−} groups, respectively. In addition, it has also been shown that pure ZrO₂ has only surface OH[−] and M–O^{2−} groups [42,43]. Therefore, it is probable that the aldol condensation reactions are catalyzed by the surface OH[−] and M–O^{2−} groups on the mixed oxides and that with an increasing amount of zirconia, there is a greater tendency to form the aldol condensation dimer, 2-methyl-2-pentenal from propanal, as shown in Table 4. In addition, an increasing amount of zirconia also leads to an increase in the yields to aromatic trimers from propanal (Table 4). This is due to an increase in the density of acid sites with increasing zirconia and the aromatization reactions being catalyzed by the acid sites [44]. This is also consistent with the results observed with γ -alumina where, 2-methyl-2-pentenal was the major observed product, with significant yields to the aromatic trimers (Table 4).

The formation of 3-pentanone over ceria–zirconia was discussed in the previous sections and is believed to proceed through the coupling of surface carboxylates. The extra oxygen necessary for this step comes from the lattice of the mixed oxide. However, 3-pentanone is also observed in the products over zirconia and γ -alumina, which are not known to be reducible like ceria or ceria–zirconia. In addition, CO₂ and H₂ were observed as the gas phase product over zirconia and γ -alumina, while only minor amounts of CO were detected. This leads to the question of the source of the extra oxygen that is required to form the carboxylates on the surface, leading to decarboxylative ketonization. Previous studies in literature have reported the possibility of the Cannizzaro reaction [51], decomposition from esters [50] and coupling

Table 4

Product distribution from conversion of propanal over Ce_xZr_{1-x}O₂ and γ -Al₂O₃ at 400 °C, 1 atm, TOS 15 min.

Feed	Propanal					
	CeO ₂	Ce _{0.75} Zr _{0.25} O ₂	Ce _{0.50} Zr _{0.50} O ₂	Ce _{0.25} Zr _{0.75} O ₂	ZrO ₂	γ -Al ₂ O ₃
W/F, h	1.02	0.42	0.36	0.22	0.038	0.36
Conversion (%)	32.7	38.4	41.5	43.8	41.8	49.0
Temperature, °C	400					
Ratio 3-pentanone/dimer	3.05	2.92	0.95	0.20	0.08	0.23
<i>Product yields (%wt)</i>						
Lights	7.9	6.9	5.6	4.7	3.6	8.7
3-Pentanone	8.4	12.3	9.0	4.7	1.7	4.6
2-Methylpentanal	1.2	2.5	2.3	3.4	2.1	3.8
2-Methyl-2-pentenal	2.7	4.2	9.4	23.3	22.5	20.3
2-Ethyl-3,5-dimethyl-2-cyclopent-2-en-1-one	0.0	0.0	0.3	1.8	3.3	4.9
1,3,5-Trimethyl benzene	0.0	0.0	0.1	0.4	1.0	1.3
2,4,6-Trimethyl phenol	0.9	0.5	0.6	0.5	0.5	0.0
Other condensation products	11.6	12.1	14.4	4.9	7.0	5.2

of carboxylates [27] as possible ways to form ketones over oxides. The possibility of forming ketones from the decomposition of an ester was tested by co-feeding 1-propanol and 1-butanol with propanal over zirconia and γ -alumina in separate experiments. The alcohol and the aldehyde are expected to form an ester on the surface through a hemiacetal intermediate with the ester subsequently decomposing to give the ketone [50]. However, the results observed here showed no significant changes in the yields of 3-pentanone in case of 1-propanol and gave only minor yields to the expected ketone, 3-hexanone with 1-butanol. This shows that the contribution of this pathway to form the ketone is minimal for the conditions of this study. If the Cannizzaro reaction is expected to proceed to form the ketone, then an enhanced formation of 1-propanol should be expected, which is also not the case here. This observation is consistent with the spectroscopic studies of benzoyl compounds on oxides by Ponc and co-workers [52], where the bands related to the expected Cannizzaro reaction products of phenylmethylketone were not observed over γ -alumina. Instead, bands assignable to methoxy and benzoate species were observed. This implies that the bond between the methyl and carbonyl group in phenylmethylketone is broken and the surface oxygen participates in the transformation of these groups to form the observed methoxy and benzoate species. In the same study, with benzaldehyde as the feed, they have also mentioned that the transformation to a surface benzoate occurs with the abstraction of hydrogen as the first step. This is then followed by the nucleophilic attack at the carbonyl group by surface oxygen to form the benzoate species. This leads to the possibility that a similar transformation is also occurring on the surfaces of zirconia and γ -alumina in this study to form 3-pentanone and thus also explaining the formation of CO_2 and H_2 that is observed in the gas phase. However, the non-reducible nature of these oxides explains the low yields of the ketones as compared to ceria or ceria-zirconia.

4. Conclusions

The following important conclusions can be drawn from the current study:

- Propanal is converted to higher carbon chain oxygenates on the ceria-zirconia catalyst by two pathways, aldol condensation and ketonization, which is in agreement with previous studies for other oxygenates and other oxide catalysts.
- The important intermediate for ketonization is a surface carboxylate formed by oxidation of the aldehyde by the oxidizing solid surface.
- The presence of acids in the feed inhibits the aldol condensation pathway by competitive adsorption of the acid that reduces the aldehyde adsorption and conversion.
- Water promotes ketonization and inhibits aldol condensation by increasing the concentration of surface hydroxyl groups that are active sites and this increases the activity by enhancing the formation of the surface carboxylates by the aldehyde.
- Catalyst stability is also increased by the presence of water.
- Hydrogen enhances cracking and produces light oxygenates and light hydrocarbons. The light oxygenates may be reincorporated to give secondary products, but the light hydrocarbons do not react further.
- Analysis of the fresh and spent catalysts by XPS showed varying degrees of reduction of the oxides under different treatment conditions that are consistent with oxide oxygen participating in the reactions.
- Changing the proportion of the parent oxides showed that increased Zr favored formation of aldol products while

increased Ce favored ketonization. This occurred by shifting the balance of the acid-base properties of the active sites.

Acknowledgements

Support from the National Science Foundation (EPSCoR 0814361), US Department of Energy (DE-FG36G088064), Oklahoma Secretary of Energy and the Oklahoma Bioenergy Center are greatly appreciated. The authors would like to thank Dr. Rolf Jentoft for the help with the X-ray diffraction measurements.

References

- P. Mckendry, Bioresour. Technol. 83 (2002) 47–54.
- C.A. Mullen, A.A. Boateng, Energy Fuels 22 (2008) 2104–2109.
- A. Corma, G.W. Huber, L. Sauvanaud, P. O' Connor, J. Catal. 257 (2008) 163–171.
- M. Gliniski, J. Kilenski, Appl. Catal. A 190 (2000) 87–91.
- K. Okumura, Y. Iwasawa, J. Catal. 164 (1996) 440–448.
- K.S. Kim, M.A. Barteau, J. Catal. 125 (1990) 353–375.
- Y. Kamimura, Y. Kamimura, S. Sato, R. Takahashi, T. Sodesawa, T. Akashi, Appl. Catal. A 252 (2003) 399–411.
- T.S. Hendren, K.M. Dooley, Catal. Today 85 (2003) 333–351.
- K.M. Dooley, A.K. Bhat, C.P. Plaisance, A.D. Roy, Appl. Catal. A 320 (2007) 122–133.
- S.D. Randery, J.S. Warren, K.M. Dooley, Appl. Catal. A 226 (2002) 265–280.
- H. Idriss, C. Diagne, J.P. Hindermann, A. Kiennemann, M. Barteau, J. Catal. 155 (1995) 219–237.
- A. Trovarelli, C. de Leitenburg, G. Dolcetti, Chemtech 27 (1997) 32–37.
- C.A. Gaertner, J.C. Serrano-Ruiz, D.J. Braden, J.A. Dumesic, J. Catal. 266 (2009) 71–78.
- P. Burroughs, A. Hammett, A.F. Orchard, G. Thornton, J. Chem. Soc., Dalton Trans. 17 (1976) 1686–1698.
- A. Trovarelli, C. de Leitenburg, M. Boaro, G. Dolcetti, Catal. Today 50 (1999) 353–367.
- J.I. Gutiérrez-Ortiz, B. de Rivas, R. López-Fonseca, J.R. González-Velasco, J. Therm. Anal. Calorim. 80 (2005) 225–228.
- G. Ranga Rao, P. Fornasiero, R. Di Monte, J. Kaspar, G. Vlaic, G. Balducci, S. Meriani, G. Gubitosa, A. Cremona, M. Graziani, J. Catal. 162 (1996) 1–9.
- C.E. Hori, H. Permana, K.Y. Simon Ng, A. Brenner, K. More, K.M. Rahmoeller, D. Belton, Appl. Catal. B 16 (1998) 105–117.
- F.B. Noronha, E.C. Fendley, R.R. Soares, W.E. Alvarez, D.E. Resasco, Chem. Eng. J. 82 (2001) 21–31.
- Jeong-Rang Kim, Wan-Jae Myeong, Son-Ki Ihm, Appl. Catal. B 71 (2007) 57–63.
- Y. Kamimura, S. Sato, R. Takahashi, T. Sodesawa, T. Akashi, Appl. Catal. A 253 (2003) 399–411.
- J.B. Claridge, M.L.H. Green, S.C. Tsang, A.P.E. York, J. Chem. Soc., Faraday Trans. 89 (7) (1993) 1089–1094.
- L. Lietti, E. Tronconi, P. Forzatti, J. Catal. 135 (1992) 400–419.
- M.M. Bettahar, G. Costentin, L. Savary, J.C. Lavalley, Appl. Catal. A 145 (1996) 1–48.
- Mark.A. Barteau, Chem. Rev. 96 (4) (1996) 1413–1430.
- L. Lietti, E. Tronconi, J. Mol. Catal. A: Chem. 94 (1994) 335–346.
- N. Plint, D. Ghavalas, T. Vally, V.D. Sokolovski, N.J. Coville, Catal. Today 49 (1999) 71–77.
- M. Kobune, S. Sato, R. Takahashi, J. Mol. Catal. A: Chem. 279 (2008) 10–19.
- O. Nagashima, S. Sato, R. Takahashi, T. Sodesawa, J. Mol. Catal. A: Chem. 227 (2005) 231–239.
- M. Renz, Eur. J. Org. Chem. 6 (2005) 979–988.
- J.C. Kuriacose, R. Swaminathan, J. Catal. 14 (1969) 348–354.
- R. Pestman, A. van Duijine, J.A.Z. Pieterse, V. Ponc, J. Mol. Catal. A: Chem. 103 (1995) 175–180.
- M. Gliniski, J. Kijenski, A. Jakubowski, Appl. Catal. A 128 (1995) 209–217.
- T. Akashi, S. Sato, R. Takahashi, T. Sodesawa, K. Inui, Catal. Commun. 4 (2003) 411–416.
- T. Yokoyama, N. Fujita, T. Maki, Appl. Catal. A 125 (1995) 159–167.
- S. Sato, R. Takahashi, T. Sodesawa, K. Matsumoto, Y. Kamimura, J. Catal. 184 (1999) 180–188.
- V.K. Diez, C.R. Apesteguia, J.I. Di Cosimo, J. Catal. 215 (2003) 220–233.
- J.I. Di Cosimo, V.K. Diez, M. Xu, E. Iglesia, C.R. Apesteguia, J. Catal. 178 (1998) 499–510.
- A. Trovarelli, Catalysis by Ceria and Related Materials, vol. 2, Imperial College Press, London, 2001.
- M.G. Cutrufflo, I. Ferino, R. Monaci, E. Rombi, V. Solinas, Top. Catal. 19 (2002) 225–240.
- E.I. Gurbuz, E.L. Kunkes, J.A. Dumesic, Appl. Catal. B 94 (2010) 134–141.
- M. Daturi, C. Binet, J. Lavalley, A. Galtayries, R. Sporcken, Phys. Chem. Chem. Phys. 1 (1999) 5717–5724.
- D. Bianchi, T. Chafik, M. Khalfallah, S.J. Teichner, Appl. Catal. A 112 (1994) 57–73.

- [44] G.S. Salvapati, K.V. Ramanamurty, M. Janardana Rao, J. Mol. Catal. 54 (1989) 9–30.
- [45] M. Daturi, E. Finocchio, C. Binet, J.C. Lavalley, F. Fally, V. Perrichon, J. Phys. Chem. B 103 (1999) 4884–4891.
- [46] J.Z. Shyu, K. Otto, W.L.H. Watkins, G.W. Graham, R.K. Belitz, H.S. Gandhi, J. Catal. 114 (1988) 23–33.
- [47] J.Z. Shyu, W.H. Weber, H.S. Gandhi, J. Phys. Chem. 92 (1988) 4964–4970.
- [48] S. Damyanova, B. Pawelec, K. Arishtirova, M.V. Martinez Huerta, J.L.G. Fierro, Appl. Catal. A 337 (2008) 86–96.
- [49] A.E. Nelson, K.H. Schulz, Appl. Surf. Sci. 210 (2003) 206–221.
- [50] M. Glinski, W. Szymanski, D. Lomot, Appl. Catal. A 281 (2005) 107–113.
- [51] H. Idriss, K.S. Kim, M.A. Barteau, J. Catal. 139 (1993) 119–133.
- [52] C.A. Kouststaal, P.A.J.M. Angevaere, V. Ponc, J. Catal. 143 (1993) 573–582.